Short Article

Structure

Palmitoylation of TEAD Transcription Factors Is Required for Their Stability and Function in Hippo Pathway Signaling

Highlights

- TEAD proteins are palmitoylated in human cells
- Palmitoylation is required for TEAD stability
- TEAD proteins do not stably associate with the nuclear envelope

Authors

Cameron L. Noland, Sarah Gierke, Paul D. Schnier, ..., Rami N. Hannoush, Wayne J. Fairbrother, Christian N. Cunningham

Correspondence

cunningham.christian@gene.com (C.N.C.), fairbrother.wayne@gene.com (W.J.F.)

In Brief

Noland et al. report that TEAD transcription factors are palmitoylated. Structures of the palmitoylated YAP-binding domains of TEAD2 and TEAD3 are presented. Palmitoylation is required for TEAD stability, highlighting a novel form of regulation of the Hippo signaling pathway.

Accession Numbers

5EMV
5EMW

Noland et al., 2016, Structure *24*, 179–186
January 5, 2016
http://dx.doi.org/10.1016/j.str.2015.11.005

Structure
Short Article

Palmitoylation of TEAD Transcription Factors Is Required for Their Stability and Function in Hippo Pathway Signaling

Cameron L. Noland,[1] Sarah Gierke,[2] Paul D. Schnier,[3] Jeremy Murray,[1] Wendy N. Sandoval,[3] Meredith Sagolla,[2] Anwesha Dey,[4] Rami N. Hannoush,[5] Wayne J. Fairbrother,[5,*] and Christian N. Cunningham[5,*]
[1]Department of Structural Biology
[2]Center for Advanced Light Microscopy
[3]Department of Protein Chemistry
[4]Department of Discovery Oncology
[5]Department of Early Discovery Biochemistry
Genentech, Inc., 1 DNA Way, South San Francisco, CA 94080, USA
*Correspondence: cunningham.christian@gene.com (C.N.C.), fairbrother.wayne@gene.com (W.J.F.)
http://dx.doi.org/10.1016/j.str.2015.11.005

SUMMARY

The Hippo signaling pathway is responsible for regulating the function of TEAD family transcription factors in metazoans. TEADs, with their co-activators YAP/TAZ, are critical for controlling cell differentiation and organ size through their transcriptional activation of genes involved in cell growth and proliferation. Dysregulation of the Hippo pathway has been implicated in multiple forms of cancer. Here, we identify a novel form of regulation of TEAD family proteins. We show that human TEADs are palmitoylated at a universally conserved cysteine, and report the crystal structures of the human TEAD2 and TEAD3 YAP-binding domains in their palmitoylated forms. These structures show a palmitate bound within a highly conserved hydrophobic cavity at each protein's core. Our findings also demonstrate that this modification is required for proper TEAD folding and stability, indicating a potential new avenue for pharmacologically regulating the Hippo pathway through the modulation of TEAD palmitoylation.

INTRODUCTION

The Hippo signaling pathway is a highly conserved kinase cascade that controls organ size and tissue homeostasis (Halder and Johnson, 2011; Zhao et al., 2011). The key downstream effectors include yes-associated protein (YAP) and its paralog, transcriptional co-activator with PDZ-binding motif (TAZ). These proteins interact with transcription factors in the nucleus to induce gene expression (Cao et al., 2008; Ota and Sasaki, 2008; Zhao et al., 2008). Upon Hippo pathway activation, Lats1/2 phosphorylates YAP, promoting its sequestration and inactivation in the cytoplasm by interaction with 14-3-3 proteins. Conversely, when this pathway is inactivated YAP is not phosphorylated and translocates into the nucleus, where it forms a complex with TEA domain (TEAD) transcription factors and co-activates the expression of multiple genes involved in cell fate determination, polarity, proliferation, and survival (Tian et al., 2010).

Defects in Hippo pathway regulation have been linked to uncontrolled cell proliferation and tumorigenesis (Harvey et al., 2013; Moroishi et al., 2015; Santucci et al., 2015). Multiple human cancers, including breast, liver, and pharyngeal cancers, show amplification or overexpression of the YAP gene (Liu et al., 2010; Overholtzer et al., 2006; Steinhardt et al., 2008; Zender et al., 2006). In addition, induced expression of YAP has been reported to trigger transformation of normal epithelial cells into metastatic cells (Overholtzer et al., 2006), and recent data have revealed that YAP is essential for the progression of pancreatic ductal adenocarcinoma in *Kras*-mutant mice (Kapoor et al., 2014). Since inhibition of the Hippo pathway leads to an activation of downstream genes, kinase components upstream of YAP phosphorylation are tumor suppressors, while YAP and TEAD, which together form a transcription co-activation complex, can promote cellular transformation. Understanding the regulation and interactions of these two proteins is therefore of critical importance to our understanding of tumorigenesis.

Crystal structures of the C-terminal YAP-binding domain (YBD) of TEAD1, TEAD2, and TEAD4 in the apo or co-activator bound states (Chen et al., 2010; Jiao et al., 2014; Li et al., 2010; Pobbati et al., 2012; Tian et al., 2010; Zhou et al., 2014) show that this domain adopts an immunoglobulin G-like fold, with two β sheets packing against each other to form a β sandwich capped with a pair of α helices (Figure 1A). The co-activator bound complex structures with YAP or vestigial-like proteins (Vgll) reveal that these proteins interact with TEAD via three distinct binding interfaces, with the majority of YAP-binding energy being driven by a short stretch of amino acids (YAP 86–100) that form a twisted-coil conformation, and bind onto a deep pocket centered around residue K289 in TEAD1.

Many proteins have been found to be regulated through S-palmitoylation, a highly conserved process occurring in all eukaryotic organisms that involves the attachment of 16-carbon fatty acids onto cysteine residues via a reversible thioester linkage (Chamberlain and Shipston, 2015; Hannoush, 2015). Palmitate

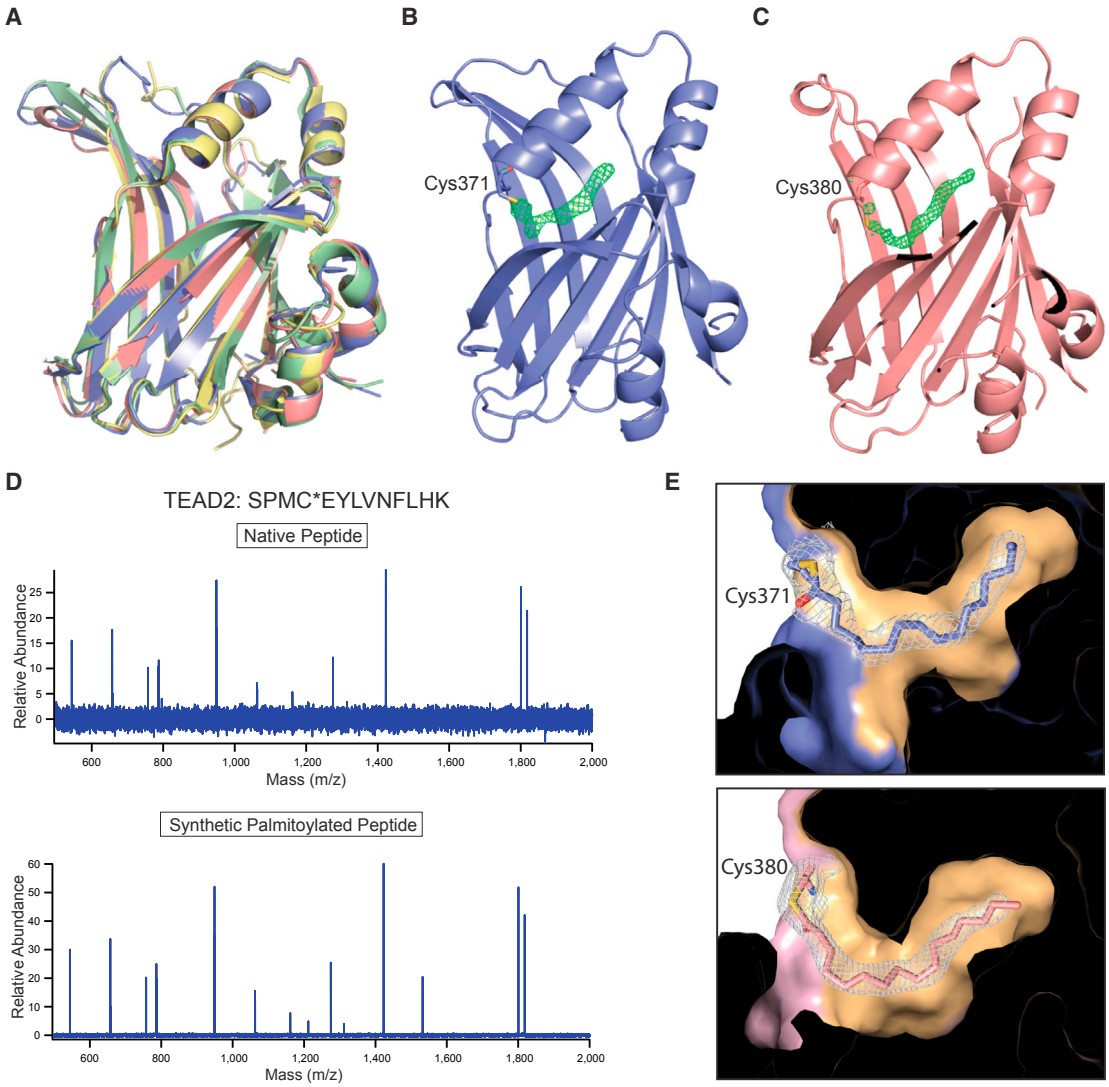

Figure 1. Structure of TEAD2 and TEAD3 Show S-Palmitoylation at a Conserved Cysteine

(A) Structural alignment of the YBDs of the four human TEAD paralogs. TEAD1-YBD (PDB: 4RE1) is shown in green. TEAD2-YBD is shown in salmon. TEAD3-YBD is shown in blue. TEAD4-YBD (PDB: 4EAZ) is shown in yellow.

(B) Crystal structure of the TEAD3-YBD with unassigned $F_o - F_c$ electron density (green mesh) contoured to 3.0σ.

(C) Crystal structure of the TEAD2-YBD with unassigned $F_o - F_c$ electron density (green mesh) contoured to 3.0σ.

(D) MS/MS spectra of the TEAD2 palmitoylated tryptic peptide (top) and a synthetic standard (bottom).

(E) Close-up view of palmitate bound within the hydrophobic TEAD3 (top) and TEAD2 (bottom) lipid-binding pockets. $2F_o - F_c$ electron density (gray mesh) is contoured to 1.0σ. Protein is shown as a surface representation with hydrophobic residues colored in orange.

See also Figure S1.

can either be added to proteins spontaneously or enzymatically by a family of DHHC motif-containing palmitoyltransferases, of which there are 23 in humans (Fukata and Fukata, 2010; Linder and Deschenes, 2007). Although there is no known consensus sequence for palmitoylation, palmitoylated cysteines share common characteristics including neighboring amino acids that are basic, a proximity to other lipidation sites, and an adjacent hydrophobic patch or core to stabilize the lipid modification (Aicart-Ramos et al., 2011; Salaun et al., 2010). Several functional consequences of protein palmitoylation have been identified, such as altered signaling or enzymatic activity, modified trafficking, increased affinity for cellular membranes, and differential stability (Linder and Deschenes, 2007).

Here we use a combination of structural, biophysical, and cell biological techniques to show that all four human TEAD homologs are S-palmitoylated in mammalian cells. Mutation of the acylated cysteine to alanine results in a complete loss of TEAD in cells, and depalmitoylation of TEAD is destabilizing, highlighting the critical nature of this adduct. Immunofluorescence microscopy in multiple mammalian cell types reveals that TEAD does not stably associate with the nuclear envelope, suggesting that the function of this modification may solely be

Table 1. Crystallographic Data Collection and Refinement Statistics

	TEAD2 (PDB: 5EMV)	TEAD3 (PDB: 5EMW)
Data Collection		
Wavelength (Å)	0.9787	0.9795
Space group	*I*121	$P2_12_12_1$
Cell dimensions		
a, *b*, *c* (Å)	79.83, 61.25, 112.67	65.31, 123.53, 150.73
α, β, γ (°)	90, 101.89, 90	90, 90, 90
Resolution (Å)	58.32–2.00 (2.05–2.00)	95.54–2.55 (2.66–2.55)
R_{merge}	0.063 (0.549)	0.109 (0.631)
Mean $I/\sigma I$	9.9 (2.0)	9.5 (2.5)
Completeness (%)	100 (100)	94.9 (96.8)
Redundancy	3.8 (3.8)	5.0 (4.9)
Refinement		
Resolution (Å)	53.54–2.00	95.54–2.55
No. of reflections	36,163 (2,696)	38,149 (4,695)
R_{work}/R_{free}	0.2053/0.2295	0.1887/0.2241
No. of atoms		
Protein	3236	6597
Ligand/ion	34	70
Water	168	167
B factors (Å^2)		
Protein	47.15	42.10
Ligand/ion	57.7	47.48
Water	48.359	43.99
Root-mean-square deviations		
Bond lengths (Å)	0.0153	0.0046
Bond angles (°)	1.294	0.845
Ramachandran plot		
Favored (%)	98.4	98.4
Allowed (%)	1.6	1.6
Outliers (%)	0	0

restricted to overall structural stability of TEAD. Together, these data reveal a novel mode of regulation for TEAD transcription factors, and ultimately Hippo signaling, suggesting a potential new approach for pharmacological intervention in diseases associated with the dysregulation of this pathway.

RESULTS

TEAD Paralogs Are Palmitoylated at a Conserved Cysteine

The four human TEAD protein YBDs (TEAD-YBDs) share an average of 73% sequence identity. TEAD2-YBD is the most divergent among these transcription factors, containing a short insertion and sharing an average pairwise identity with the YBDs of other human TEAD paralogs of 67%. Several crystal structures have been reported characterizing the YBDs of human TEAD1, TEAD2, and TEAD4 proteins in either the apo state or in complex with YAP or Vgll proteins (see below). We sought to structurally characterize TEAD3-YBD and, to this end, crystallized the protein and solved the structure to 2.55 Å resolution (Table 1, Figure 1B). As expected, TEAD3-YBD shares the same overall fold as other TEAD-YBD paralogs. An alignment of the TEAD3-YBD Cα carbons to TEAD1-YBD (PDB: 4RE1), TEAD2-YBD (discussed below), and TEAD4-YBD (PDB: 4EAZ) structures gave root-mean-square deviations of 0.509, 0.445, and 0.535 Å, respectively (Figure 1A). The overall TEAD3-YBD fold is composed primarily of two adjacent β sheets that are splayed at one end to create a hydrophobic cavity capped by two α helices. At the entrance to this cavity lies a universally conserved cysteine residue (C371). To our surprise, we found significant $F_o - F_c$ electron density resembling that of an aliphatic chain in this hydrophobic pocket that was connected directly to C371 (Figure 1B). Interestingly, upon solving the structure of the TEAD2-YBD to 2.00 Å resolution, a similar $F_o - F_c$ electron density was present and connected to C380 (Table 1, Figure 1C). Given the shape of the density, its location in a hydrophobic pocket, and its proximity to a conserved surface cysteine, we surmised that TEAD3 and TEAD2 are likely lipidated. Since these proteins were obtained by expression in *Escherichia coli*, which lacks palmitoyltransferases, we hypothesize that these proteins undergo a spontaneous, non-catalytic lipidation when expressed in bacterial cells.

To confirm the identity of the additional electron density in our structures, we used intact and tandem mass spectrometry (MS/MS) analysis of the bacterially expressed TEAD2-YBD. The deconvoluted mass spectrum of intact TEAD2-YBD shows two predominant masses of 30,402.20 Da and 30,640.31 Da (Figure S1A). The 238-Da difference is consistent with a palmitate modification. The presence of a non-palmitoylated mass is likely due to reducing reagent in our purification; however, we believe that palmitate is likely still non-covalently present in the TEAD2-YBD hydrophobic pocket in this species based on experiments described below. Peptide mapping experiments were performed to identify the site of palmitoylation in TEAD2-YBD, and three cysteine-containing tryptic peptides were identified using a C18 column (DTQELLLCTAYVFEVSTSER; VCSFGK; SPMCEYLVNFLHK). Selected ion-monitoring experiments were subsequently performed using direct infusion of the TEAD2-YBD digest to look for S-palmitoylated versions of the three detected cysteine-containing peptides. A singly protonated tryptic peptide at *m/z* 1818.9721 consistent with the palmitoylated peptide SPMCpEYLVNFLHK (3 ppm mass error) was observed (Figure S1B). To further reinforce that the 238-Da mass addition is due to a palmitoylation event, we synthesized a palmitoyl peptide standard by performing a palmitoylation reaction on the synthetic peptide SPMCEYLVNFLHK (see Supplemental Experimental Procedures). The MS/MS spectra of the tryptic peptide from the TEAD2-YBD digest (Figure 1D, top) and the synthetic standard (Figure 1D, bottom) are superimposable, providing unequivocal evidence that TEAD2-YBD is S-palmitoylated at C380.

Based on these findings, we modeled an S-palmitoylated cysteine into the unexpected electron densities in our crystal structures at C380 of TEAD2-YBD and C371 of TEAD3-YBD (Figure 1E). The *B* factors for these ligands are similar to those of the proteins as a whole (Table 1), albeit slightly higher, potentially due to the presence of reducing reagent in our protein purifications and thermal motion of the palmitate within the lipid-binding site. The hydrophobic residues forming the TEAD lipid-binding

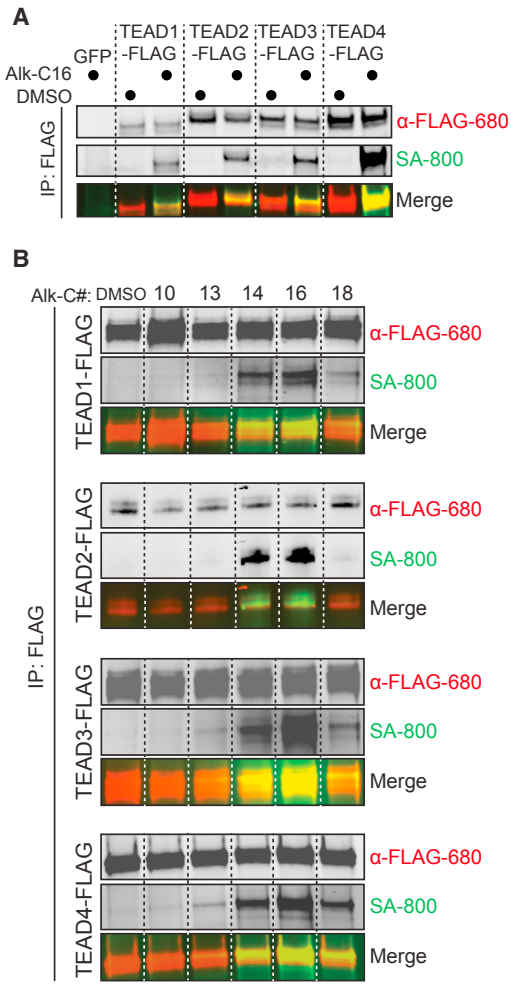

Figure 2. Mammalian Expressed TEADs Are Palmitoylated

(A) Metabolic labeling of TEAD paralogs with Alk-C16 chemical probes in HEK293T cells. α-FLAG-680 and SA-800 are antibodies directed against the FLAG tag of TEAD or biotinylated fatty acid, respectively.

(B) Alkyne modified fatty acids of varying length were incubated on HEK293T cells transfected with each of the four TEAD paralogs. Alk-C# denotes the number of carbons on each fatty acid.

IP, immunoprecipitation. See also Figure S2.

site are highly conserved among all TEAD paralogs, with only five residues diverging in one of the four family members (Figure S1C). However, despite this conservation, lipidation of the YBD of TEAD proteins has not previously been reported. This finding led us to reexamine the electron density maps for every publicly available TEAD-YBD crystal structure to look for possible lipid electron density (Figure S1D). This analysis revealed that a similar electron density is present to varying degrees in every TEAD-YBD crystal structure deposited to date. Differing levels and types of reducing agents used to purify TEAD-YBD proteins, as well as potentially varying levels of lipid flexibility within the binding pocket, likely account for differences in palmitate site occupancy between each study and within our own experiments. In sum, our structural and MS studies of TEAD protein YBDs indicate that these proteins are palmitoylated at C344 of TEAD1, C380 of TEAD2, C371 of TEAD3, and C360 of TEAD4.

TEAD Paralogs Are Palmitoylated in Mammalian Cells

As our structural work used bacterially expressed proteins, we sought to confirm that the TEAD paralogs are also palmitoylated in mammalian cells. Using previously established methods (Gao and Hannoush, 2014; Hannoush, 2012; Hannoush and Arenas-Ramirez, 2009) we metabolically labeled transiently expressed C-terminally FLAG-tagged full-length TEAD paralogs or GFP (as a control) in HEK293T cells with a clickable ω-alkynyl palmitate analog (Alk-C16) (Figure S2A). A FLAG immunoprecipitation was performed, and the alkyne-labeled palmitoylated proteins were chemoselectively ligated to biotin by a Cu(1)-catalyzed alkyne-azide [3 + 2] Huisgen cycloaddition reaction. Anti-FLAG AlexaFluor 680 antibody and streptavidin-IRDye 800 were used to monitor TEAD and palmitoylation status, respectively, using western blot analysis. In corroboration of our structural characterization, we found that all four TEAD paralogs are palmitoylated in mammalian cells (Figure 2A). Using alkynyl fatty acid analogs of various chain lengths in a similar assay, we observed that C16 fatty acid chains were the most preferred across all four TEAD proteins, but that C14 (myristoyl) fatty acids were also incorporated, with C13 and C18 lipid lengths observed to a much lesser and variable extent (Figure 2B).

TEAD Palmitoylation Is Not Dynamic and Is Required for Protein Stability

Recent studies focused on understanding the dynamics of palmitoylation show that addition and removal of this modification is important for the regulation of protein localization, protein stability, and fine-tuning the activity of proteins, analogous to phosphorylation or ubiquitination (Salaun et al., 2010). For example, the Ras cycling pathway uses cycles of palmitoylation and depalmitoylation to regulate its localization in the cell and, subsequently, its signaling function (Rocks et al., 2005). To determine the rate of turnover of TEAD2 palmitoylation in mammalian cells, we used a pulse-chase approach with Alk-C16. HEK293T cells transiently transfected with full-length TEAD2-FLAG were pulse labeled with Alk-C16 overnight and then chased with complete medium lacking Alk-C16 over the course of 48 hr. The depalmitoylation rate of TEAD was very slow during the time course, with a 40% reduction of palmitoylation observed after the 48-hr chase period (Figures 3A and 3B). These data suggest that TEAD palmitoylation is not dynamic but rather most likely co-exists with the protein throughout its lifetime until its ultimate degradation. The irreversible nature of TEAD S-palmitoylation is rather uncharacteristic for S-palmitoylated proteins due to the reversible and dynamic nature of the thioester bond, and is more analogous to that of Wnt proteins, which are O-palmitoylated (Gao and Hannoush, 2014), and Hedgehog proteins, which are N-palmitoylated (Buglino and Resh, 2012).

To investigate the functional role of TEAD palmitoylation, we mutated either the palmitoylated cysteine or an adjacent conserved lysine residue located 6.6 Å away from the cysteine (as measured from the sulfur atom of the cysteine to the lysine ε-amino group), and analyzed protein steady-state levels (Figures S3A and S3B). We reasoned that this lysine residue might lower the pK_a of the cysteine and thereby enable spontaneous palmitoylation. Full-length wild-type, C380A, or K357A TEAD2-FLAG were transiently transfected into HEK293T cells. Cells were lysed and separated into soluble and insoluble fractions,

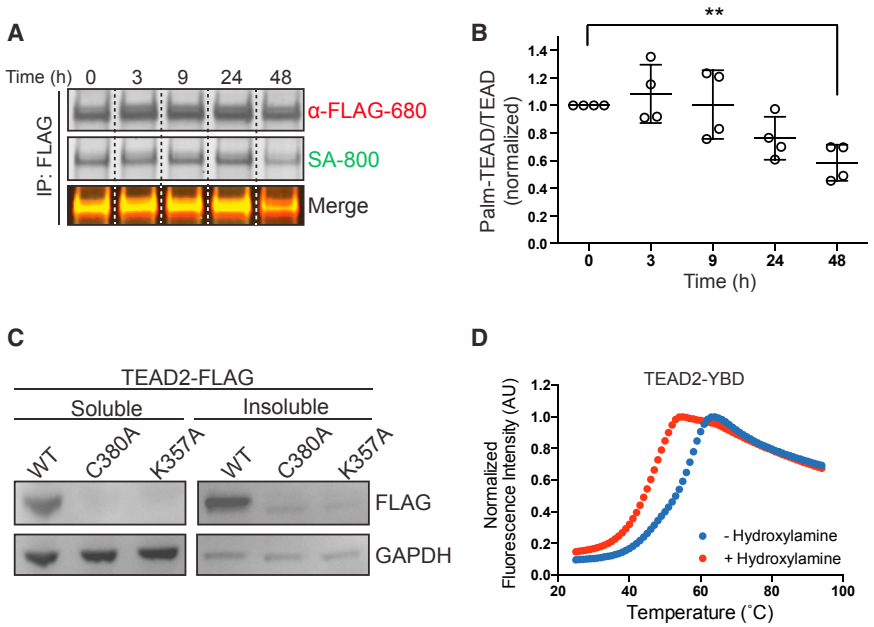

Figure 3. Palmitoylation of TEAD Is Required for Stability

(A) Palmitoylation turnover measurements for full-length TEAD2 using an overnight Alk-C16 pulse followed by a chase with unmodified complete medium over five time points.

(B) Quantification of fraction of palmitoylated TEAD2 from (A). Each point represents the ratio of a single experiment with SA-800 band intensity (palm-TEAD) measured versus α-FLAG-680 (TEAD) band intensity at each time point. Error bars represent SD of n = 4 experiments with significance reported (**$p < 0.01$ by two-way ANOVA and Dunnett's multiple comparison test).

(C) Western blot protein-level analysis of full-length TEAD2 wild-type, C380A, and K357A constructs in HEK293T cells. Cells were fractionated into soluble and insoluble fractions and blotted against FLAG and GAPDH.

(D) Thermal denaturation curves for TEAD2-YBD (blue) and TEAD2-YBD that has been treated with hydroxylamine (red). Data represent the averages of three separate measurements. Error bars represent SD of n = 3.

See also Figure S3.

and subjected to SDS-PAGE and western blot analysis using antibodies against the FLAG tag or GAPDH as a loading control (Figure 3C). Interestingly, both the C380A and K357A mutant TEAD2 proteins displayed a substantial loss of overall protein levels when compared with the wild-type protein. We believe the enriched amount of wild-type protein found in the insoluble fraction may be attributed to overexpressed TEAD2 that is present in the nucleus, since the lysis procedure does not break up the nuclear membrane.

The loss of TEAD2 when either C380 or K357 are mutated to alanine suggested that palmitoylation is required for protein stability. To test this directly we treated TEAD2 with hydroxylamine, a strong reducing agent known to specifically cleave thioester bonds at neutral pH. We then measured the thermal stabilities of the treated and non-treated forms of TEAD2 by differential scanning fluorimetry. Despite the possibility that the palmitate may still be non-covalently bound in the lipid-binding pocket of the hydroxylamine-treated protein, this analysis showed a dramatic decrease in T_m from 61.1 ± 0.2°C for the palmitoylated protein, to 48.8 ± 0.8°C for the hydroxylamine-treated protein (Figure 3D), demonstrating that TEAD palmitoylation stabilizes the protein.

TEAD Is Not Stably Associated with the Nuclear Envelope

Since palmitoylation increases the hydrophobicity of cytoplasmic proteins, this post-translational modification has been shown to promote their association, permanently or temporarily, with cholesterol- and sphingolipid-rich lipid rafts (Brown, 2006; Yang et al., 2010). Because TEAD is a transcription factor, we hypothesized that its palmitoylation may function to localize it onto the nuclear envelope. We used immunofluorescence and confocal microscopy to assess the subcellular localization of native TEAD in four mammalian tumor cell lines: a model cervical cancer cell line, HeLa; a YAP overexpressing colon cancer cell line, OUMS-23; and two pancreatic tumor-derived cell lines with either YAP overexpression or TEAD4 amplification, SW-1990 and PATU-8902, respectively. All cell lines were grown in chamber slides for 24 hr before fixing, permeabilizing, and incubating with antibodies against pan-TEAD and a nuclear pore component protein, NUP98, to serve as a nuclear envelope marker (see Experimental Procedures). In all four cell lines we observe a diffuse TEAD staining located exclusively throughout the nucleoplasm, with little to no staining detected in the cytoplasm (Figures 4 and S4). In contrast, NUP98 displays a diffuse staining pattern throughout the nucleus, with the highest signal intensity observed in a ring around the nucleus, corresponding to the nuclear envelope of the cell. When the fluorescence patterns of NUP98 and TEAD are compared with one another no appreciable co-localization is observed, leading us to conclude that TEAD is not stably associated with the nuclear envelope under these equilibrium-based conditions.

DISCUSSION

As the furthest downstream regulators in the Hippo signaling pathway, TEAD transcription factor stability is of critical importance to cell growth and proliferation. We have solved the first structure of the TEAD3-YBD, demonstrating its high level of structural similarity to the analogous domains of other human TEAD-YBDs. More importantly, our structural studies of the TEAD2- and TEAD3-YBDs have identified an S-palmitoylation site on TEAD proteins. To date, the importance of protein S-palmitoylation has centered on the fact that it is a reversible hydrophobic modification, the presence or absence of which can affect the localization, function, and regulation of proteins dynamically throughout the cell cycle. Surprisingly, S-palmitoylation of TEAD does not seem to alter protein localization and/or association to a membrane surface, leading us to conclude that TEAD either does not interact with the nuclear envelope or any other membrane-bound organelle or, if it does, the association rate is too fast to measure under equilibrium conditions. Instead, our thermal stability data indicate that TEAD palmitoylation is

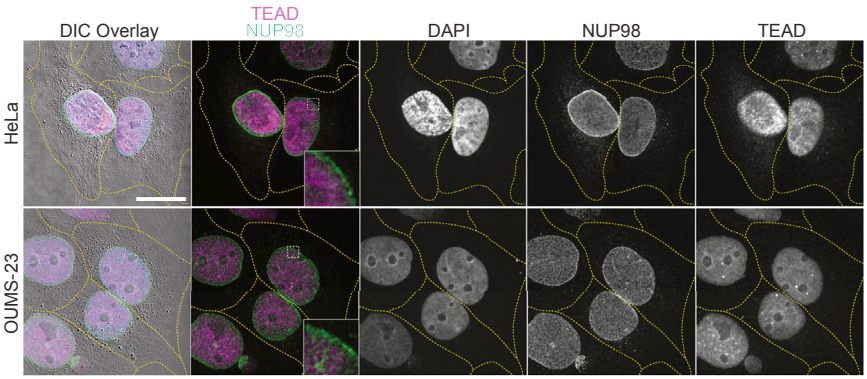

Figure 4. Immunofluorescence of Native TEAD and NUP98 in Tumor Cell Lines

Cells were fixed and stained for TEAD (magenta), NUP98 (green), and DNA (DAPI, blue) in HeLa and OUMS-23 cells. DIC overlay includes DIC and all fluorescent channels. Insets show indicated regions at higher magnification. All images represent a single confocal optical section. Yellow dotted lines represent cell boundaries. Scale bar represents 20 μm. See also Figure S4.

directly responsible for the overall stability of the protein. There are a handful of studies showing that, at least in part, palmitoylation contributes to overall protein stability. For example, palmitoylation of the A_1 adenosine G-protein-coupled receptor protects newly synthesized proteins from being proteolytically cleaved and subsequently degraded, with an apparent 9-fold reduction in half-life of the non-palmitoylated receptor (Gao et al., 1999).

Most current drug discovery efforts have focused on trying to antagonize the TEAD-YAP interaction through their protein-protein interface (Liu-Chittenden et al., 2012; Santucci et al., 2015; Zhou et al., 2014). It remains to be seen whether the interplay between the palmitoylation of TEAD and the various degradation pathways of cells may prove to be an attractive strategy for therapeutic intervention in the Hippo pathway. Intriguingly, it has been demonstrated recently that the TEAD central pocket is targetable with small molecules such as flufenamic acid and its analogs. These molecules inhibit the transcription of genes normally upregulated during YAP overexpression without affecting the TEAD-YAP interaction (Pobbati et al., 2015). Although the exact mechanism of TEAD inhibition by flufenamic acid has not been determined, in light of the present findings it seems likely that these molecules displace the palmitate from the hydrophobic core, which may lead to destabilization of TEAD proteins in vivo.

Fully understanding how TEAD is palmitoylated in mammalian systems will be essential for understanding the regulation and dynamics of this essential signaling pathway. With proteomic efforts and technological advances rapidly uncovering the complete human palmitoylated proteome (Chamberlain and Shipston, 2015; Hannoush, 2015), it is becoming increasingly evident that being able to modulate the lipidation state of many proteins will be fundamental to understanding their function and regulation in a vast assortment of cellular processes. Importantly, these efforts will, in many cases, have direct relevance to the development and success of new therapeutic strategies.

EXPERIMENTAL PROCEDURES

Protein Expression and Purification

TEAD2-YBD (A217-D447) and TEAD3-YBD (Q216-D435) constructs containing tobacco etch virus protease-cleavable N-terminal His tags were expressed in *E. coli* BL21 (DE3) cells by autoinduction and purified by standard purification techniques for His-tagged proteins (see Supplemental Experimental Procedures for details).

Crystallization

TEAD2-YBD crystals of the body-centered monoclinic space group *I*121 were grown at 19°C by hanging-drop vapor diffusion using a drop ratio of 2:1 protein/reservoir solution. Reservoir solution contained 100 mM Tris (pH 7.3) and 1.7–2.1 M sodium formate. Crystals were cryoprotected in reservoir solution supplemented with 25% glycerol.

TEAD3-YBD crystals of the primitive orthorhombic space group $P2_12_12_1$ were also grown at 19°C by hanging-drop vapor diffusion using a drop ratio of 2:1 protein/reservoir solution. Reservoir solution contained 100 mM sodium acetate (pH 4.5), 100 mM calcium acetate, and 12% polyethylene glycol 4000. Crystals were cryoprotected in reservoir solution supplemented with 30% glycerol.

Data Collection and Structure Determination

X-Ray diffraction data were collected for TEAD2-YBD and TEAD3-YBD crystals at beamlines 21-ID-F at the Advanced Photon Source and 5.0.2 at the Advanced Light Source, respectively. Data were processed using iMosflm (Battye et al., 2011). The TEAD2-YBD structure was solved by molecular replacement using Phaser (McCoy et al., 2007), with the previously published TEAD2-YBD structure (Tian et al., 2010) as a search model and two molecules in the asymmetric unit. The structure was then rebuilt in Coot (Emsley and Cowtan, 2004), and subjected to iterative rounds of refinement and rebuilding using Phenix (Adams et al., 2010) and Coot. Data processing and refinement statistics are summarized in Table 1. Clear extra density at C380 was modeled as an S-palmitoyl cysteine for each molecule in the asymmetric unit.

The structure of TEAD3-YBD was also solved by molecular replacement using Phaser, with an unpalmitoylated version of our TEAD2-YBD structure as the search model and four molecules in the asymmetric unit. The structure was then rebuilt manually in Coot using the TEAD3-YBD sequence as a guide, and subjected to iterative rounds of refinement and rebuilding using Phenix and Coot. Data processing and refinement statistics are summarized in Table 1. Clear extra density at C371 was modeled as an S-palmitoyl cysteine for each molecule in the asymmetric unit.

Metabolic Lipid Labeling, Click Chemistry, and Visualization of TEAD

Alkyne fatty acid labeling was performed as described previously (Gao and Hannoush, 2014; Hannoush, 2012; Hannoush and Arenas-Ramirez, 2009). A detailed description of this and our western blotting analysis protocols are described in Supplemental Experimental Procedures.

Immunofluorescence Imaging

HeLa, PaTu-8902, OUMS-23, or SW-1990 cells were plated on poly-lysine-coated eight-well chamber cells at 20,000 cells/well. Following 24 hr of growth, cells were fixed with 4% paraformaldehyde in PBS at pH 7.4. Following permeabilization (0.1% Triton X-100 in PBS), blocking (2% BSA in PBS), and primary antibody incubation (1:100 dilution), antibodies were visualized using Alexa dye-conjugated secondary antibodies (1:1,000 dilution). Images were collected on a Nikon A1R confocal microscope with a 100 × 1.45 Plan Apo oil-immersion objective. Alexa 488 and Alexa 647 were imaged with the 488 and 640 laser lines, respectively. The differential interference contrast (DIC) image was collected simultaneously with the 488 laser. DIC images presented in Figures 4 and S4 were processed with shading correction (background flexibility, 30; signal, average) and unsharp mask (power, 0.5; area, 5), using

NIS-Elements Imaging Software (Nikon) to correct for light variation across images and enhanced contrast to better visualize cell outlines.

ACCESSION NUMBERS

The accession numbers for the TEAD2 and TEAD3 structures reported in this paper are PDB: 5EMV and 5EMW, respectively.

SUPPLEMENTAL INFORMATION

Supplemental Information includes Supplemental Experimental Procedures and four figures and can be found with this article online at http://dx.doi.org/10.1016/j.str.2015.11.005.

AUTHOR CONTRIBUTIONS

C.L.N., S.G., P.D.S., M.S., and C.N.C. were responsible for the experimental work. C.L.N., P.D.S., A.D., R.N.H., W.J.F., and C.N.C. planned the project and designed the experiments. All authors analyzed the data. C.L.N. and C.N.C. wrote the manuscript with help from all authors.

ACKNOWLEDGMENTS

The authors acknowledge D. Barnes, T. Hagenbeek, X. Gao, C. Klijn, and N. Skelton for their helpful discussions related to this work. The authors declare competing financial interests: all authors are employees of Genentech, Inc.

Received: September 16, 2015
Revised: November 9, 2015
Accepted: November 24, 2015
Published: December 24, 2015

REFERENCES

Adams, P.D., Afonine, P.V., Bunkóczi, G., Chen, V.B., Davis, I.W., Echols, N., Headd, J.J., Hung, L.-W., Kapral, G.J., Grosse-Kunstleve, R.W., et al. (2010). PHENIX: a comprehensive Python-based system for macromolecular structure solution. Acta Crystallogr. D Biol. Crystallogr. *66*, 213–221.

Aicart-Ramos, C., Valero, R.A., and Rodriguez-Crespo, I. (2011). Protein palmitoylation and subcellular trafficking. Biochim. Biophys. Acta *1808*, 2981–2994.

Battye, T.G.G., Kontogiannis, L., Johnson, O., Powell, H.R., and Leslie, A.G.W. (2011). iMOSFLM: a new graphical interface for diffraction-image processing with MOSFLM. Acta Crystallogr. D Biol. Crystallogr. *67*, 271–281.

Brown, D.A. (2006). Lipid rafts, detergent-resistant membranes, and raft targeting signals. Physiology (Bethesda) *21*, 430–439.

Buglino, J.A., and Resh, M.D. (2012). Palmitoylation of Hedgehog proteins. Vitam. Horm. *88*, 229–252.

Cao, X., Pfaff, S.L., and Gage, F.H. (2008). YAP regulates neural progenitor cell number via the TEA domain transcription factor. Genes Dev. *22*, 3320–3334.

Chamberlain, L.H., and Shipston, M.J. (2015). The physiology of protein S-acylation. Physiol. Rev. *95*, 341–376.

Chen, L., Chan, S.W., Zhang, X., Walsh, M., Lim, C.J., Hong, W., and Song, H. (2010). Structural basis of YAP recognition by TEAD4 in the hippo pathway. Genes Dev. *24*, 290–300.

Emsley, P., and Cowtan, K. (2004). Coot: model-building tools for molecular graphics. Acta Crystallogr. D Biol. Crystallogr. *60*, 2126–2132.

Fukata, Y., and Fukata, M. (2010). Protein palmitoylation in neuronal development and synaptic plasticity. Nat. Rev. Neurosci. *11*, 161–175.

Gao, X., and Hannoush, R.N. (2014). Single-cell imaging of Wnt palmitoylation by the acyltransferase porcupine. Nat. Chem. Biol. *10*, 61–68.

Gao, Z., Ni, Y., Szabo, G., and Linden, J. (1999). Palmitoylation of the recombinant human A1 adenosine receptor: enhanced proteolysis of palmitoylation-deficient mutant receptors. Biochem. J. *342* (Pt 2), 387–395.

Halder, G., and Johnson, R.L. (2011). Hippo signaling: growth control and beyond. Development *138*, 9–22.

Hannoush, R.N. (2012). Profiling cellular myristoylation and palmitoylation using ω-alkynyl fatty acids. Methods Mol. Biol. *800*, 85–94.

Hannoush, R.N. (2015). Synthetic protein lipidation. Curr. Opin. Chem. Biol. *28*, 39–46.

Hannoush, R.N., and Arenas-Ramirez, N. (2009). Imaging the lipidome: omega-alkynyl fatty acids for detection and cellular visualization of lipid-modified proteins. ACS Chem. Biol. *4*, 581–587.

Harvey, K.F., Zhang, X., and Thomas, D.M. (2013). The Hippo pathway and human cancer. Nat. Rev. Cancer *13*, 246–257.

Jiao, S., Wang, H., Shi, Z., Dong, A., Zhang, W., Song, X., He, F., Wang, Y., Zhang, Z., Wang, W., et al. (2014). A peptide mimicking VGLL4 function acts as a YAP antagonist therapy against gastric cancer. Cancer Cell *25*, 166–180.

Kapoor, A., Yao, W., Ying, H., Hua, S., Liewen, A., Wang, Q., Zhong, Y., Wu, C.-J., Sadanandam, A., Hu, B., et al. (2014). Yap1 activation enables bypass of oncogenic Kras addiction in pancreatic cancer. Cell *158*, 185–197.

Li, Z., Zhao, B., Wang, P., Chen, F., Dong, Z., Yang, H., Guan, K.-L., and Xu, Y. (2010). Structural insights into the YAP and TEAD complex. Genes Dev. *24*, 235–240.

Linder, M.E., and Deschenes, R.J. (2007). Palmitoylation: policing protein stability and traffic. Nat. Rev. Mol. Cell Biol. *8*, 74–84.

Liu, A.M., Xu, M.Z., Chen, J., Poon, R.T., and Luk, J.M. (2010). Targeting YAP and Hippo signaling pathway in liver cancer. Expert Opin. Ther. Targets *14*, 855–868.

Liu-Chittenden, Y., Huang, B., Shim, J.S., Chen, Q., Lee, S.-J., Anders, R.A., Liu, J.O., and Pan, D. (2012). Genetic and pharmacological disruption of the TEAD-YAP complex suppresses the oncogenic activity of YAP. Genes Dev. *26*, 1300–1305.

McCoy, A.J., Grosse-Kunstleve, R.W., Adams, P.D., Winn, M.D., Storoni, L.C., and Read, R.J. (2007). Phaser crystallographic software. J. Appl. Crystallogr. *40*, 658–674.

Moroishi, T., Hansen, C.G., and Guan, K.-L. (2015). The emerging roles of YAP and TAZ in cancer. Nat. Rev. Cancer *15*, 73–79.

Ota, M., and Sasaki, H. (2008). Mammalian Tead proteins regulate cell proliferation and contact inhibition as transcriptional mediators of Hippo signaling. Development *135*, 4059–4069.

Overholtzer, M., Zhang, J., Smolen, G.A., Muir, B., Li, W., Sgroi, D.C., Deng, C.-X., Brugge, J.S., and Haber, D.A. (2006). Transforming properties of YAP, a candidate oncogene on the chromosome 11q22 amplicon. Proc. Natl. Acad. Sci. USA *103*, 12405–12410.

Pobbati, A.V., Chan, S.W., Lee, I., Song, H., and Hong, W. (2012). Structural and functional similarity between the Vgll1-TEAD and the YAP-TEAD complexes. Structure *20*, 1135–1140.

Pobbati, A.V., Han, X., Hung, A.W., Weiguang, S., Huda, N., Chen, G.-Y., Kang, C., Chia, C.S.B., Luo, X., Hong, W., et al. (2015). Targeting the central pocket in human transcription factor TEAD as a potential cancer therapeutic strategy. Structure *23*, 2076–2086.

Rocks, O., Peyker, A., Kahms, M., Verveer, P.J., Koerner, C., Lumbierres, M., Kuhlmann, J., Waldmann, H., Wittinghofer, A., and Bastiaens, P.I.H. (2005). An acylation cycle regulates localization and activity of palmitoylated Ras isoforms. Science *307*, 1746–1752.

Salaun, C., Greaves, J., and Chamberlain, L.H. (2010). The intracellular dynamic of protein palmitoylation. J. Cell Biol. *191*, 1229–1238.

Santucci, M., Vignudelli, T., Ferrari, S., Mor, M., Scalvini, L., Bolognesi, M.L., Uliassi, E., and Costi, M.P. (2015). The hippo pathway and YAP/TAZ-TEAD protein-protein interaction as targets for regenerative medicine and cancer treatment. J. Med. Chem. *58*, 4857–4873.

Steinhardt, A.A., Gayyed, M.F., Klein, A.P., Dong, J., Maitra, A., Pan, D., Montgomery, E.A., and Anders, R.A. (2008). Expression of Yes-associated protein in common solid tumors. Hum. Pathol. *39*, 1582–1589.

Tian, W., Yu, J., Tomchick, D.R., Pan, D., and Luo, X. (2010). Structural and functional analysis of the YAP-binding domain of human TEAD2. Proc. Natl. Acad. Sci. USA *107*, 7293–7298.

Yang, W., Di Vizio, D., Kirchner, M., Steen, H., and Freeman, M.R. (2010). Proteome scale characterization of human S-acylated proteins in lipid raft-enriched and non-raft membranes. Mol. Cell. Proteomics *9*, 54–70.

Zender, L., Spector, M.S., Xue, W., Flemming, P., Cordon-Cardo, C., Silke, J., Fan, S.-T., Luk, J.M., Wigler, M., Hannon, G.J., et al. (2006). Identification and validation of oncogenes in liver cancer using an integrative oncogenomic approach. Cell *125*, 1253–1267.

Zhao, B., Ye, X., Yu, J., Li, L., Li, W., Li, S., Yu, J., Lin, J.D., Wang, C.-Y., Chinnaiyan, A.M., et al. (2008). TEAD mediates YAP-dependent gene induction and growth control. Genes Dev. *22*, 1962–1971.

Zhao, B., Tumaneng, K., and Guan, K.-L. (2011). The Hippo pathway in organ size control, tissue regeneration and stem cell self-renewal. Nat. Cell Biol. *13*, 877–883.

Zhou, Z., Hu, T., Xu, Z., Lin, Z., Zhang, Z., Feng, T., Zhu, L., Rong, Y., Shen, H., Luk, J.M., et al. (2014). Targeting Hippo pathway by specific interruption of YAP-TEAD interaction using cyclic YAP-like peptides. FASEB J. *29*, 724–732.

